DARPA Zenith
Ferro-fluid Ionic Liquid Mirror (FILM)
Optical Modeling & Simulation Report

PROJECT NO.
EG-006610
(75111)

CDRL#: A005

Document Number: RPT-75111-1000

Prepared By:	**Neil Rowlands**
Function:	**Engineer Fellow**
Prepared By:	**Sheng-Hai Zheng**
Function:	**Optical Engineering**
Approved By:	**Rebecca Kamire**
Function	**Lead R&D Engineer / Scientist**
Approved By:	**Amanda Childers**
Function:	**Project Manager**
Date:	**June 27, 2024**

DARPA Program #: HR0011366236
For ARFL Contract #: FA237724CB011

CAGE CODE: 99193

CM RELEASE DATE

REV. 1

DOCUMENT REVISION RECORD

Pages not listed remain at the released revision level.
Pages affected by the current ECN reflect the present document revision level.

Revision Level	ECN Number	Date	Checked By	CM Release	Pages Affected
0		APRIL 8, 2024	NR		Initial Release
1		JUNE 27, 2024	NR		Update for completion of Phase I

Table of Contents

List of Figures

List of Tables

1. INTRODUCTION

1.1 PURPOSE

This report provides a summary of the optical portion of the Modeling & Simulation activities undertaken to fulfil the requirements of the DARPA Zenith Liquid Mirror Telescope project. This report, along with the accompanying technical report on ferro-fluidic modeling from Georgia Tech, is intended to satisfy the deliverable A005 Technical Information Report as per the CDRL list, Attachment 3 to [AD-2]. These reports are part of the '8-month' Phase I milestone as per [AD-1]:

> *"Delivery M&S results and Version 1 of proprietary and non-proprietary computer code. Deliverable to include Open-source M&S codes developed during Phases I and II, to include user-friendly manuals and well-documented instructions for use. All computer code delivery must include in-code comments, instructions for use, and any other code documentation, embodying all results to date, for IV&V verification that quality of simulations is meeting/not meeting program needs."*

The source code accompanying these reports (ie. Version 1) is delivered separately, but is also attached in Section 4.4.1. This computer code delivery includes in-code comments, while the reports provide the overarching instructions for their use, references to other documentation, and provides examples of use and all significant results to date. Together with the source codes these reports are intended to provide DARPA with the ability to perform independent verification and validation of the simulations.

This version 1 document is an update of the version 0, mainly replacing the 2D analytical model results with the 3D version and updating the optical modeling results.

1.2 BACKGROUND

The original concept proposed to fulfil the DARPA Zenith requirement has been maintained in this project, namely a design incorporating a curved Halbach array to provide a uniform magnetic field which maintains the surface shape of composite ionic liquid ferro-fluid magnetic which in turn produces a mirror surface of sufficient imaging quality [AD-3]. Initially it was hoped that the residual magnetic non-uniformity from the Halbach array could be (intrinsically) minimized, while also providing a strong enough magnetic field for the ferro-fluid to maintain a highly accurate shape despite the varying gravity vector due to the off-axis pointing requirements.

In fact, neither goal could be achieved with the Halbach design alone and the PDR concept has evolved to include both a passive correction of the residual periodic variations in the magnetic field produced by the Halbach array, and an active correction of the larger scale shape variation induced by the shifting gravity vector due to tilting. Using the models described here, these two perturbations were balanced to derive the nominal PDR design and the required level of correction derived.

1.3 REPORT FORMAT

This optical modeling report is divided into two main sections, the first provides a summary of the results taken as the current baseline from the ferro-fluid modeling accomplished to date, along with a listing of the main conclusions from this modeling which has informed the PDR design. The second section covers the optical modeling which was undertaken to assess the impact of the ferro-fluidic model scenarios on the potential optical quality of a mirror formed with these model shapes.

2. REFERENCES

2.1 APPLICABLE DOCUMENTS

[AD-1] BAA HR001123S0021
[AD-2] AFRL Contract FA2377-24-C-B011
[AD-3] Honeywell Proposal & Statement of Work OPRO-0033901
[AD-4] DARPA Zenith Phase-I Software Technical Report (LGST-2024-001) Ver. 0, April 4th, 2024
[AD-5] DARPA Zenith Phase-I Ferrohydrodynamic M&S Software Technical Report (LGST-2024-001) Ver. 1, June 27th, 2024

2.2 REFERENCE DOCUMENTS

[RD-1] K. Halbach, Applications of permanent magnets in accelerators and electron storage rings, Journal of Applied Physics 57 (1). doi:10.1063/1.335021.
[RD-2] Mallinson, J. C., “One-Sided Fluxes — A Magnetic Curiosity?,” IEEE Trans. Magn., 9, 678–682 1973. https://doi.org/10.1109/TMAG.1973.1067714.
[RD-3] A. Romero-Calvo, G. Cano-G´omez, H. Schaub, Diamagnetically enhanced electrolysis and phase separation in low gravity, AIAA Journal of Spacecraft and Rockets 59 (1) (2021) 1–13. https://doi.org/10.2514/1.A35021.
[RD-4] Wetherell, W. B.; "Effects Of Mirror Surface Ripple On Image Quality," *Proc. SPIE 0332, Advanced Technology Optical Telescopes I*, 1982. https://doi.org/10.1117/12.933538.

2.3 ACRONYMS

AFRL	Air Force Research Laboratory
BAA	Broad Agency Announcement
CDRL	Contract Data Requirements List
DARPA	Defense Advanced Research Projects Agency
FILM	Ferro-fluid Ionic Liquid Mirror
IL	Ionic Liquid
IV&V	Independent Verification and Validation
M&S	Modeling and Simulation
PDR	Preliminary Design Review
P-V	Peak-to-Valley
RMS	Root Mean Square
WFE	Wavefront Error

3. FERRO-FLUID MAGNETIC MODELING

3.1 BACKGROUND

The ferro-fluid magnetic modeling is described in detail in separate reports [AD-4] & [AD-5]. Some of the key assumptions and results are summarized here. The objective of this phase of this project is to demonstrate via modeling and simulation how a ferro-fluid mirror in conjunction with a Halbach array may be used to achieve the DARPA program objectives of a 0.5 m demonstration mirror which can produce acceptable image quality while being pointed up to 10° off-axis.

A Halbach array is a particular arrangement of permanent magnets that produces one-sided magnetic fields [RD-1]. The Mallinson magnetic configuration from which it derives [RD-2] generates equipotential lines that become quasi-parallel to its surface [RD-3] overcoming the force of gravity for a ground-based liquid mirror telescope through the adjustment of internal magnetic configurations – as shown schematically in Figure 3-1. The nominal ferro-fluid being investigated in this project is a combination of two immiscible ionic liquids which will self-assemble into a bi-layer arrangement with a thick ferro-fluid layer on the bottom and a thin layer containing reflective nanoparticles on the top. The details of these fluids will be discussed in other project reports. The optical requirements on the top layer are discussed in section **Error! Reference source not found.** of this report.

In the proposal [AD-3] it was identified that mid-frequency wavefront error would be a significant contribution to image quality because of the intrinsic variation of the magnetic field generated by discrete magnets. Initial surveys of the parameter space, described in section 2 of [AD-4], initially revealed that smaller magnets (for example 1/8" in size) could suppress the mid-frequency variations on the ferro-fluid surface to under 200 nm peak-to valley. However subsequent 2D modeling of titled flat Halbach arrays using the analytical methods described in section 3 of [AD-4], revealed that the change in the overall shape of the surface (the global WFE) when tilted would be better controlled, ie. have a smaller amplitude, with larger magnets.

This was then the fundamental trade-off for this project, to minimize the shape change due to tilting a method would have to be found to correct for larger mid-frequency WFE. Fortunately, as shown in section 3.2.4, this mid-frequency WFE is almost completely independent of the tilting, meaning that a fixed passive correction of the Halbach array magnetic field is possible, for example by applying a thin layer of variable permeability material between the Halbach array and the ferro-fluid.

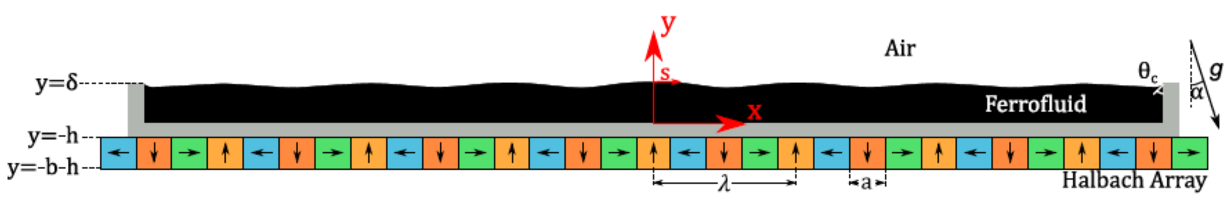

Figure 3-1. Conceptual Halbach Array with Ferro-fluid

3.2 ANALYTICAL MODELS

The optical model results described in this report (in Section **Error! Reference source not found.**) are based on the ferrofluidic analytical model described in Section 4 '3D Spherical Global Tilting' of [AD-5], but before the two dimensional tilting and ferrofluid density variation was implemented. [AD-4]The differences are described below and some data from the Version 1 ferrofluid model is shown in below.

3.2.1 Baseline Parameters

The Matlab function (*main.m*) sets up and calls the suite of functions that form this '3D Spherical Global Tilting' model. Table 3-1 compares the three main sets of baseline simulation parameters that were used.

Table 3-1 Ferro-fluid model parameters used for optical modeling

Parameter	Version 0	'Version 0.5' (Section 4)	Version 1 (Section 3.2)	Description
xf	0.25	0.25	0.25	Surface half length (m)
delta	0.001	**0.002**	**0.002**	Fluid height (m)
sigma	61.7×10^{-3}	61.7×10^{-3}	61.7×10^{-3}	Surface tension (N/m)
Alpha	10 x pi/180	10 x pi/180	**15 x pi/180**	Array tilt inclination (rad) (the tilt angle was varied)
Beta	n/a	n/a	**15 x pi/180**	Array tilt inclination (rad) (the tilt angle was varied)
Ms	4000	**10,000**	**5607 or 8000**	Saturation magnetization (A/m)
R	2	2	2	Spherical Mirror surface radius (m)
A	0.5	0.5	0.5	Spherical mirror surface aperture (m)
w	½ * 0.0254	½ * 0.0254	½ * 0.0254	Width of individual magnets (m)
t	0	0	0	Separation between magnets (m)
b	1*0.0254	1 * 0.0254	1*0.0254	Height of individual magnets (m)
L	0.25	**0.3**	**0.3**	Half-length of Halbach array (m)
h	0.004	**0.009**	**0.009**	Separation between Halbach array and fluid (m)
M0	1177.7×10^{-3}	1177.7×10^{-3}	1177.7×10^{-3}	Magnet magnetization (A/m)
D0	-0.0515	**-0.077**	**-0.0515**	Vertical displacement of center of array (m) (note1)
Rm	R+h+b/2+delta+d0			Magnet array radius at centerline of the array (m)
shim_c	0.01	0.01	0.01	Passive correction of Halbach ripple (note 2)
DNoN	n/a	n/a	**0.2**	Variation in ferrofluid density in percent

Notes to Table 3-1:

1) the effective shape of the Halbach array is adjusted by this fixed offset to account for the nominal fluid displacement as a function of radius due to the varying gravity vector over the nominal curved surface. This ensures the desired spherical shape is achieved with no active correction required when the mirror tilt is 0°.
2) this correction factor is used to model the passive correction which will be employed to reduce the ripple induced by the Halbach array – the details of the implementation and modeling of this correction will be incorporated into the next version of these reports.

The typical parameters varied in this simulation were the tilt angle and the passive correction factor. The latter is a reduction factor applied to the mid-frequency ripple determined in the simulation.

The second column of Table 3-1 lists the parameters used in the 2D analytic ferrofluid model to provide the results analyzed in Version 0 of this report. The third column lists the parameters used in the 3D analytical model whose output was then optically modeled as described in section 4 below. The fourth column lists the parameters available in Version 1 of the analytical ferrofluid model described in Section 4 '3D Spherical Global Tilting' of [AD-5]. This model now includes tip & tilt in two dimensions and a parameter to account for density variations in the ferrofluid. While the outputs of this updated model have not yet been evaluated in an optical model, sections 3.2.3, 3.2.4 & 3.2.5, provide examples of the outputs and describe their potential impacts on the optical models.

3.2.2 Baseline 2D Results: Global Shape

With the baseline parameters listed in the Version 0 column of Table 3-1, the 2D analytical curved model with tilt provides the surface shapes shown in Figure 3-2. The deviation from the ideal spherical shape is not immediately apparent but becomes apparent after subtraction of the best fit sphere as shown in Figure 3-3. Note that there is also residual linear slope (discussed in more detail below) which has also been removed.

Also shown in Figure 3-2 and Figure 3-3 is the baseline without any passive correction factor applied. In particular Figure 3-3 shows that the relative amplitude of the deviations from ideal shape on the low (or global) spatial frequency scale vs the deviations on the mid-frequency scale (dotted lines). These contributions are comparable because of the magnet size selected for the baseline. As can be seen good performance of the passive correction will be essential to achieving the optical performance, ie. the correction needed is a factor 100 or better. Similar performance will need to be achieved in the active correction which will correct for the low spatial frequency spatial shape changes with tilting.

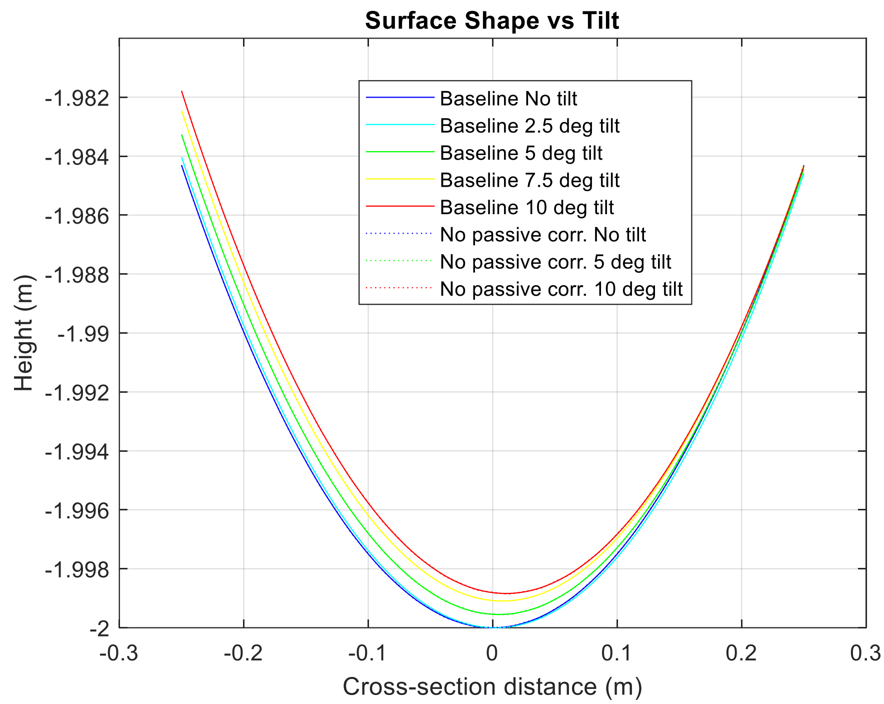

Figure 3-2 Baseline Surface Shape vs Tilt Angle

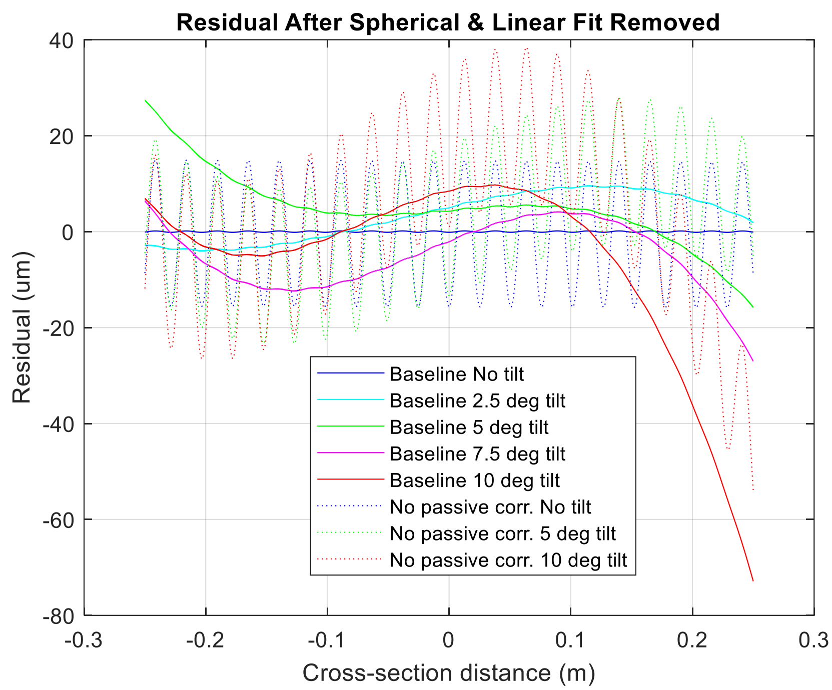

Figure 3-3 Baseline Surface Residual vs Tilt Angle

3.2.3 Baseline 3D Results: Global Shape

Some results from the updated 3D analytical ferrofluid model are described here, in this case using the parameters from the fourth column of Table 3-1. To compare these results to the previous ones, the new ferrofluid density parameter was set to zero, see section 3.2.5 for the impact of this density factor on the mid-frequency ripple. This is the most up-to-date model and includes primary mirror tilting in two axes. This is included here to demonstrate that the global shape induced by tilting is consistent with the earlier 2D analytical results and both the PDR results and the results described in section 4.2, using the 3D analytical model with tilting in one dimension. Figure 3-4 shows a surface height map of residuals after fitting a tilted spherical surface to the model output for a ferrofluid with a saturation magnetization of 8000A/m. The tilt angles listed in the figure captions are applied to both axes. The color scales indicated are in microns, and this scale expands as the tilt angles increase. The non-tilted case shows only the mid-frequency ripple. The shape of the Halbach array is set such that an ideal spherical shape is obtained with zenith pointing.

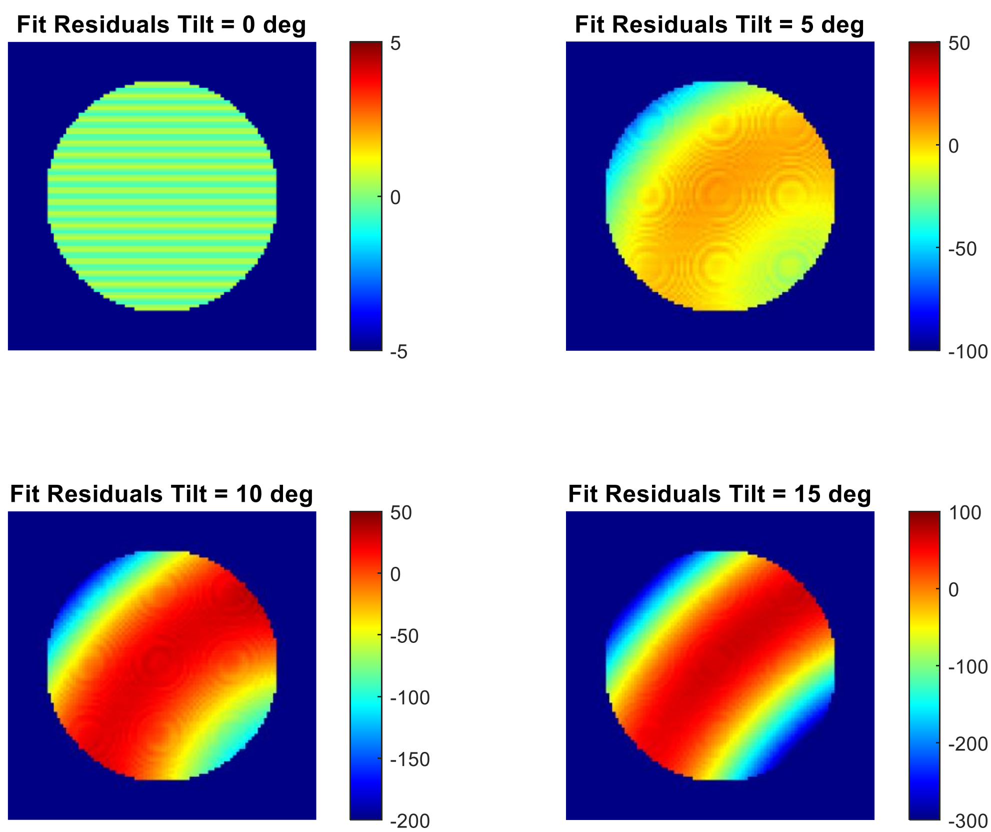

Figure 3-4 Residual Surface Profiles after spherical & tip/tilt fits.

Table 3-2 Fitted Spherical & Linear Surface Parameters

		Fitted Parameters (offsets, radius & slopes) in mm				
Ms (A/m)	tilt angle	xo	yo	R-2m	slope x	slope y
8000	0	0	0	0	0	0
	5	1.10	1.20	0.30	-0.75	-0.78
	10	3.30	-2.90	-2.10	-1.63	-0.88
	15	1.80	0.80	-3.40	-1.98	-1.93

Table 3-2 lists the parameters for the surfaces fitted to the ferrofluid model output vs tilt angles, in this case the tilt angle is in both axes. The change in best fit spherical radius will be accommodated in the system by a focus adjustment. The change in slope however requires compensation at the primary mirror otherwise it would cause bulk flow of the fluid, ie. change in fluid thickness as a function of tilt angle. This can be compensated by tilting the dish with respect to the Halbach array as the overall off-zenith pointing of the system is changed. The slope values in Table 3-2 are shown as mm of change at the edge of the 0.5m mirror. For the case of a pointing off-zenith of 15° in both axes, this represents a change in the dish to Halbach array of just under 0.5 compared to the zenith orientation. This will be managed by a small dish tilting system mounted on the Halbach array support structure.

3.2.4 Baseline Results: Mid-Frequency Ripple

Another key result of this initial modeling is the demonstration that the mid-frequency ripple from the Halbach array is independent of the tilting under gravity. To check/confirm this with the updated ferrofluid model, the model output discussed in the previous section was evaluated by plotting the difference between the shape profiles with and without the passive correction, for a given tilt angle as shown in Figure 3-5. This is done by differencing the ferrofluid model output with the 'shim_c' parameter set to its nominal 0.01 and with this parameter set to zero. Figure 3-6 plots a vertical cross section of this surface profile difference data. There is essentially no change with tilt angle in the mid-frequency surface profile induced by the Halbach array discretization.

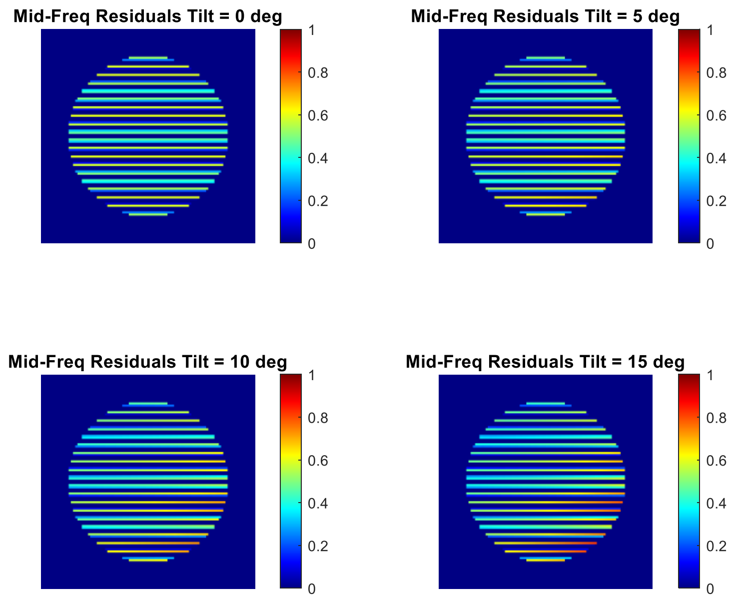

Figure 3-5 Difference in the shape profiles with passive correction to 1% and with perfect correction

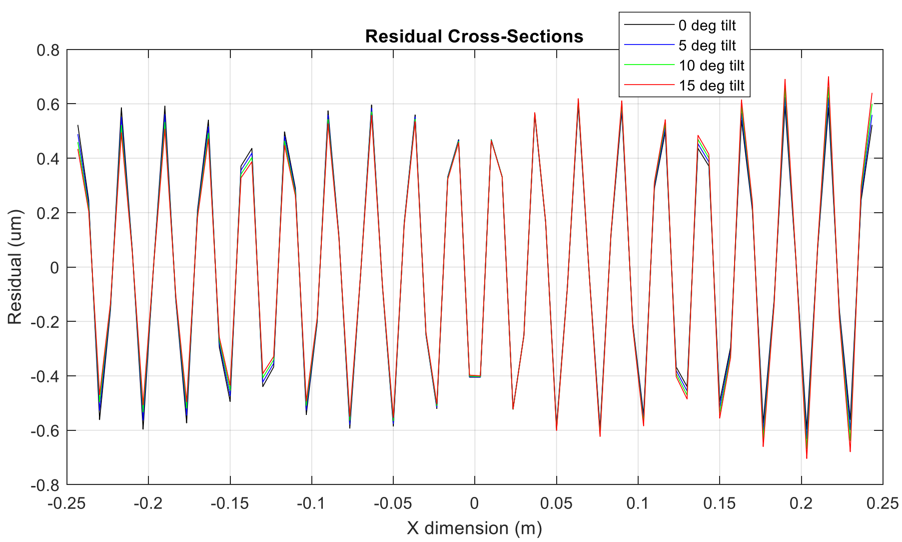

Figure 3-6 Differences the cross-section of the shape profile with passive correction to 1% and with perfect correction

3.2.5 Baseline Results: Ferrofluid Density Variation

The other new feature of the Version 1 ferrofluid analytical code is the inclusion of a parameter to account for the observed variations in ferrofluid density. The best current estimate for the percentage variation is 20%. As a preliminary assessment of the impact, the model was run with no variation and with a 20% variation, as shown in Figure 3-7. In this example the saturation magnetization was 5607 A/m and the tilt angle in both axes was 10°. There is no apparent difference in the global shape induced by tilting, however taking the difference of model output with and without the passive correction reveals the impact on the mid-frequency ripple as shown in Figure 3-8. In both cases show the passive correction factor is assumed to be 0.01. Compared to Figure 3-6 (with a slightly different Ms) the impact of a 20% variation in ferrofluid density causes the mid-frequency ripple to increase by about a factor of 10 and this will place more demands on the passive correction.

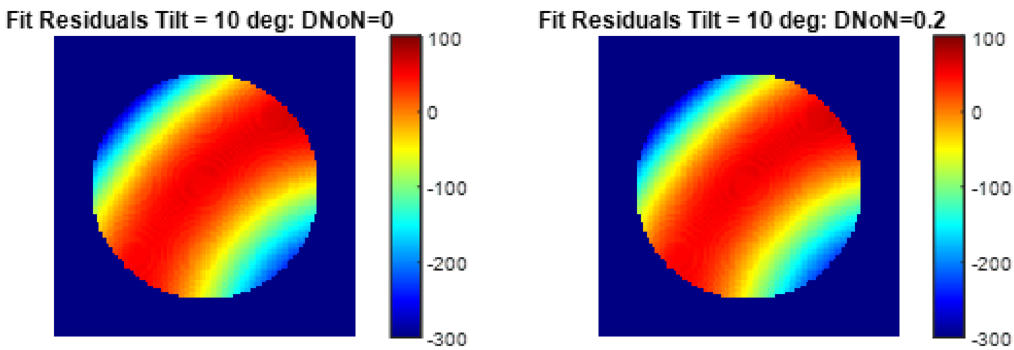

Figure 3-7 Residual Surface Profiles after spherical & tip/tilt fits: Ms = 5607A/m

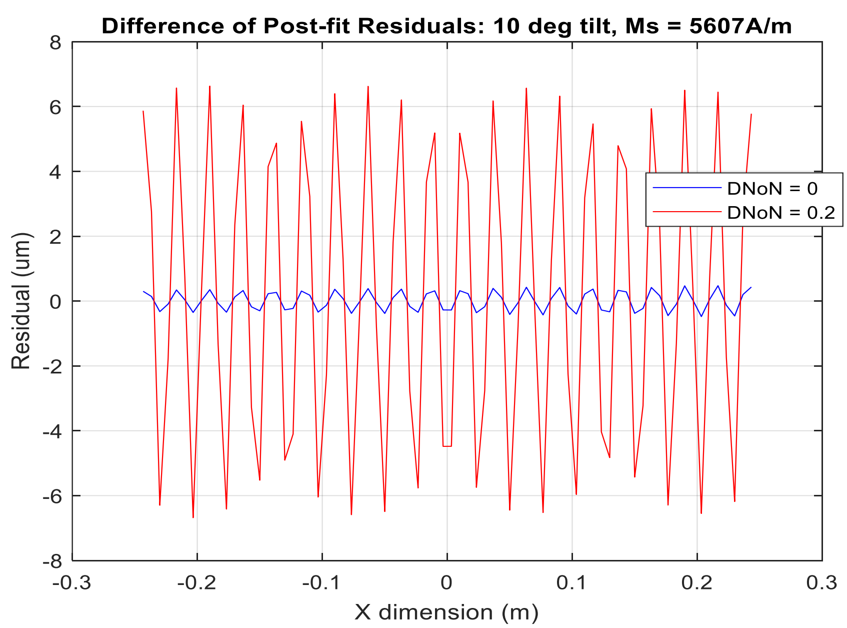

Figure 3-8 Impact of Ferrofluid Density Variation of Mid-Frequency Ripple

3.3 3D COMSOL FINITE ELEMENT ANALYSIS

A true 3-dimensional simulation of the magnetic flux density generated by the Halbach array requires a finite element analysis which is possible using the commercial FEA code COMSOL Multiphysics®. This model is still under development with some preliminary results obtained as described in section 5 of [AD-5]. This model will include simulation of the passive and active control. In order to incorporate these results into the optical modeling, the coupled COMSOL MATLAB model described in section 6 of [AD-5] will be used and the results included in future versions of this optical modeling report.

4. OPTICAL MODELING

4.1 BACKGROUND

Early ferro-fluidic modeling demonstrated that this design concept presents a tradeoff between mid-frequency wavefront error induced by nature of the Halbach array and the deviation of the fluid surface from its ideal shape due to the influence of a changing gravity vector when the array and mirror are tilted together.

The initial results from the 2D ferrofluidic modeling described in the previous version of this report resulted in the selection of ½" form factor magnets for the Halbach array. The 2D models were then used to assess the performance for the nominal mirror concept proposed for Phase II, a 0.5m clear diameter spherical mirror with a nominal radius of curvature of 2m. In this updated version of the optical modeling report this performance assessment has been updated using the results from the 3D ferrofluid model described in the previous section.

4.2 OPTICAL MODELING PROCESS

The fluid surface deviations from the ideal spherical shape provided by the ferrofluid modeling were imported to optical modeling software to assess their impact on the image quality (wavefront error and Strehl ratio). The following steps were followed:

1) Remove the base radius by calculating a best fit sphere and differencing the model output from the fit.
2) Remove piston, tip and tilt by fitting for x,y,z offsets and slopes in x & y (mx & my).
3) Model the resulting surface figure by 5th order Zernike fitting – this is the global (low-frequency) WFE – an example is shown in Figure 4-1 (left).
4) Obtain a residual which is the mid-frequency WFE – an example is shown in Figure 4-1 (right).
5) Scale the global WFE contribution and add to the optical prescription as a Zernike Standard Sag surface.
6) Scale the mid-frequency residual and add to the optical prescription as a Grid Sag surface.
7) Apply the top liquid layer as a wedged refractive element on top of the reflective surface (so it contributes as a double pass). The wedge is to account for a uniform gradient in top layer thickness that is expected as the mirror is tilted. This top layer is conservatively assumed to 'fill-in' the mid-frequency surface profile due to the Halbach array, with the top surface otherwise following the nominal global surface shape.

Table 4-1 lists the ZEMAX OpticStudio surface types used, these two SAG surfaces are applied to the same prescription file to obtain the results.

Table 4-1 Optical Modeling Process Breakdown

Spatial Frequency	Zemax Modeling	Effect
Low Frequency	Zernike Standard SAG Surface	Conventional aberration
Middle Frequency	Grid SAG Surface	Small angle scattering that blurs image
High Frequency	Scattering or coating	Wide-angle scattering treated as loss to be included in the reflectivity assessment

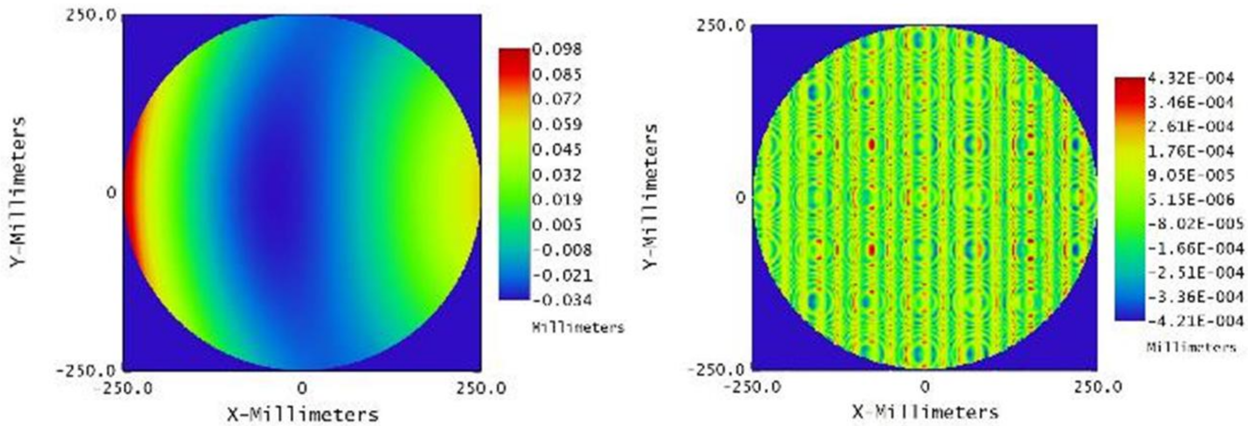

Figure 4-1 Examples of the Zernike Standard Sag surface (to model the global WFE) and the Grid Sag surface (to model the mid-frequency WFE).

4.3 WAVEFRONT ERROR BUDGET

To establish how much passive and active correction will be required, ie. to establish the scale factors that need to be applied to the mid-frequency and global (low frequency) WFE in order to achieve a functional primary mirror, a preliminary wavefront error budget can be used. The nominal budget shown in Table 4-2 assigns the same WFE requirement to each major contributor and will be used to assess the scale factors required.

Table 4-2 RMS wavefront error budget allocation

	WFE in units of λ at 550 nm		
	Low	Mid	Total
Top layer	0.080	0.080	0.113
Ferrofluid layer	0.080	0.080	0.113
		Total	0.160
		Requirement (λ/6 at 550 nm)	0.167
		Margin (RMS)	0.047

4.4 SETTING THE CORRECTION REQUIREMENTS

With the RMS WFE targets set by the budget in Table 4-2, the required level of passive and active correction can be determined from the surface profiles output by the ferrofluid models. For example RMS and peak-to-valley deviations from the ideal spherical surface is shown in the middle columns of Table 4-3, for a ferrofluid saturation magnetization of 10,000 A/m, a fluid thickness of 1 mm and a fluid height of 9 mm above the Halbach array. These values are the physical deviation from ideal of the equipotential surface obtained by the ferrofluid model described in section 3. Note that these factors do not yet include the impact of the ferrofluid density variation.

The shape profiles provided by the ferrofluid model are fitted as described above to determine the nominal best fit spherical radius, piston error and tip / tilt. This produces wavefront error maps which are then scaled by the required correction factors to obtain the WFE maps shown in Figure 4-2. These correction factors are listed in the last column of Table 4-3. The contributions of the transmissive top layer to the WFE are modeled simply as a refractive element which follows the profile of the ferrofluid layer. This effectively amplifies the impact of the mid-frequency ripple. There is also an allowance for the top layer to have a wedge or variation in layer thickness from one side of the mirror to the other of 0.5mm. This will induce an image shift which can be corrected (or accounted for) downstream, but also contributes some WFE.

Considering all these contributions, the resulting total RMS WFE meets the $\lambda/6$ at λ=550 nm requirement while the effective Strehl ratio is ~0.35. Note that the correction factor for the mid-frequency reduction is the total, including the factor of 100 from the ferrofluid model and an additional 35x to bring its WFE contribution in line with the budget shown in Table 4-2.

Table 4-3 Correction factors for Ms=10,000 A/m

WFE contributor	Spatial scale	Conditions	Physical surface sag before correction		Required correction factor
			Peak to valley (µm)	RMS (µm)	
Ferrofluid	**Mid-freq**	2k scale	457	77	3500
	Global	10° tilt	43	8	365
Top layer	**Mid-freq**	As per ferrofluid surface 1 mm nominal thickness			
	Global	0.5 mm uniform thickness 'wedge' at 10° tilt			

The correction of the global wavefront error induced by tilting is expected to be done via active control of the magnetic field at the primary mirror, but it should be noted that the global wavefront error is well fitted by a set of 5th order Zernike polynomials which does indicate that this wavefront could also potentially be corrected downstream, i.e. after the primary mirror, with a deformable mirror system. This would be an alternative to active control of the magnetic field at the primary mirror, concepts for which are in development.

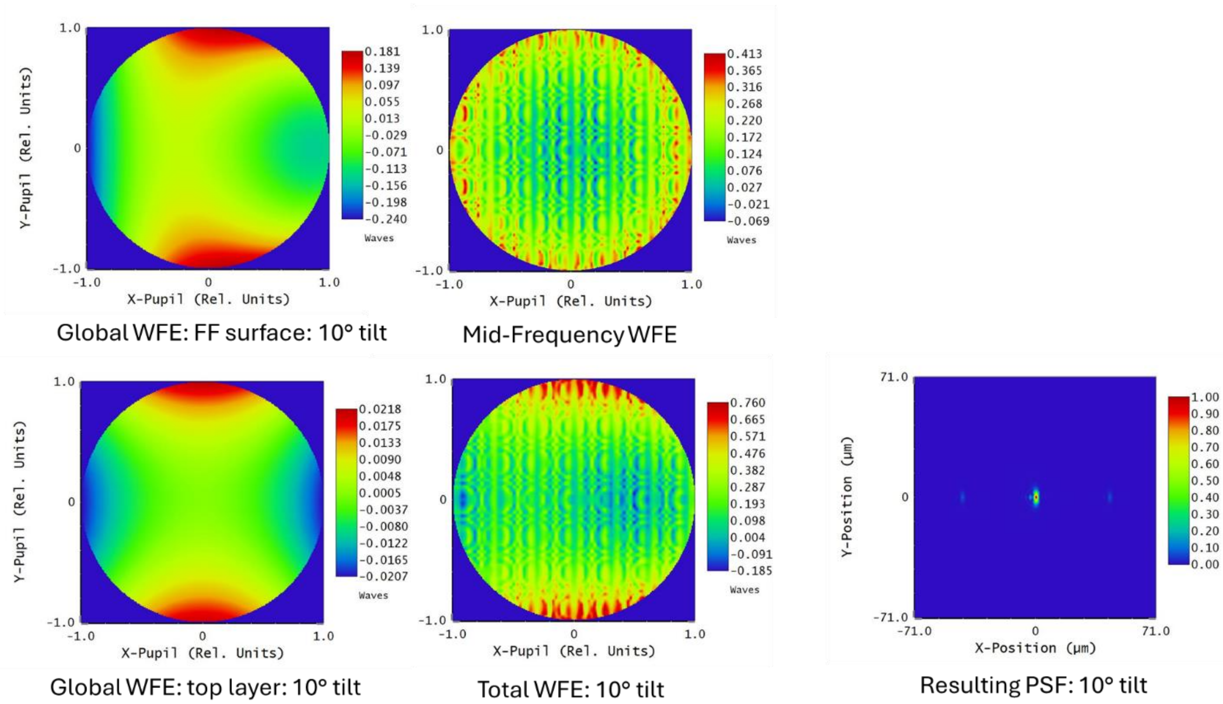

Figure 4-2 WFE Maps: scaled global WFE due to tilt (top left), the scaled mid-frequency WFE due to the Halbach array (top middle), the global WFE due to the wedge of the top layer (bottom left), the total combination of these (bottom middle) and the resulting point spread function (bottom right).

4.4.1 Prescription Files

The ZEMAX OpticsStudio prescription files used to obtain the results presented in this section are provided as a ZEMAX archive file: 'Zenith_FILM_Optical_V1.zar' attached here:

Zenith_FILM_Optical_
V1.zar

5. SUMMARY

The modeling and simulation described in this report have provided the basis for the following key design decisions for the nominal Phase II baseline for the demonstration of a 0.5m FILM:

A) Larger individual Halbach array magnets minimize the variation in global shape under tilting but come at the expense of larger amplitude residual Halbach array ripple impacting mid-frequency wavefront error. The selected design concept balances these two contributions.
B) As a result of A) a passive correction is added to the design which provides a stationary magnetic field correction to the Halbach array, the required reduction of this ripple pattern intrinsic to the Halbach array is to ~0.01% of its uncorrected amplitude, now that ferrofluid density variations have been included.
C) Also, because of A) an active correction is added to the design which provides a means to dynamically adjust the magnetic field, correcting the global WFE induced by off-axis tilting of the mirror. The required reduction of these low order Zernike shape changes is to ~0.8% of their uncorrected amplitudes. Fortunately, the shape changes are at low spatial frequencies, requiring only low resolution active control.
D) The impact of the top layer is now included in the same optical model which uses the ferrofluid model output to define the reflective layer profile. An allowance has been made for a simple variation in thickness of this top layer and this will be used to help target the chemical properties of this liquid layer.